NASA TECHNICAL MEMORANDUM

NASA TM X-2405

NASA TM X-2405

EXPERIMENTAL INVESTIGATION OF THE PERFORMANCE OF VORTEX GENERATORS MOUNTED IN THE SUPERSONIC PORTION OF A MIXED-COMPRESSION INLET

by Glenn A. Mitchell

Lewis Research Center
Cleveland, Ohio 44135

NATIONAL AERONAUTICS AND SPACE ADMINISTRATION • WASHINGTON, D. C. • NOVEMBER 1971

1. Report No.	2. Government Accession No.	3. Recipient's Catalog No.
NASA TM X-2405		

4. Title and Subtitle	5. Report Date
EXPERIMENTAL INVESTIGATION OF THE PERFORMANCE OF VORTEX GENERATORS MOUNTED IN THE SUPERSONIC PORTION OF A MIXED-COMPRESSION INLET	November 1971
	6. Performing Organization Code

7. Author(s)	8. Performing Organization Report No.
Glenn A. Mitchell	E-6418
	10. Work Unit No. 764-74

9. Performing Organization Name and Address	11. Contract or Grant No.
Lewis Research Center National Aeronautics and Space Administration Cleveland, Ohio 44135	

12. Sponsoring Agency Name and Address	13. Type of Report and Period Covered
National Aeronautics and Space Administration Washington, D. C. 20546	Technical Memorandum
	14. Sponsoring Agency Code

15. Supplementary Notes

16. Abstract

Vortex generators were investigated as a means of controlling the throat boundary layer in a Mach 2.5 mixed-compression inlet. With or without throat bleed, the generators were unable to produce the inlet peak recoveries available with good performance bleed. Generators placed on the unbled inlet centerbody ahead of the cowl shock impingement point degraded inlet performance. Generators placed further aft on the unbled centerbody, but ahead of the throat, improved inlet performance at conditions where the terminal shock could cause boundary-layer separation. Adding generators to the inlet with throat bleed reduced performance. Bleed aft of the generators degraded the vortex flow field.

17. Key Words (Suggested by Author(s))	18. Distribution Statement
Vortex generators in supersonic flow Boundary-layer control Supersonic mixed-compression inlets	Unclassified - unlimited

19. Security Classif. (of this report)	20. Security Classif. (of this page)	21. No. of Pages	22. Price*
Unclassified	Unclassified	37	$3.00

* For sale by the National Technical Information Service, Springfield, Virginia 22151

EXPERIMENTAL INVESTIGATION OF THE PERFORMANCE OF VORTEX GENERATORS MOUNTED IN THE SUPERSONIC PORTION OF A MIXED-COMPRESSION INLET

by Glenn A. Mitchell

Lewis Research Center

SUMMARY

Vortex generators were investigated as a means of boundary-layer control in the supersonic portion of a mixed-compression inlet. The generators were located on the inlet centerbody ahead of the cowl shock impingement point, aft on the centerbody ahead of the throat, and on the cowl ahead of the throat. The test was conducted in the Lewis 10- by 10-Foot Supersonic Wind Tunnel at a Mach number of 2.5.

Either with or without throat bleed the vortex generators were unable to produce inlet peak recovery levels as high as those available with a good boundary-layer bleed system. Generators placed on the inlet centerbody ahead of the cowl shock impingement point degraded the unbled boundary layer and decreased inlet total-pressure recovery by 1 percent. Generators aft of this centerbody location but ahead of the inlet throat improved the unbled boundary layer. Total-pressure recovery was increased about 1 percent and distortion was reduced about 1 percent. These gains were realized only at conditions where the inlet terminal shock was capable of causing the turbulent boundary layer to separate.

Cowl and aft centerbody vortex generators in combination with throat bleed reduced the inlet total-pressure recovery as much as 3.5 percent. Bleed regions immediately aft of vortex generators degraded the vortex flow field.

Centerbody vortex generators ahead of the inlet throat were incapable of providing effective control of the subsonic-diffuser boundary layer.

INTRODUCTION

Inlets of conventional design rely on bleed to remove the low-energy boundary layer ahead of the throat and obtain acceptable levels of inlet pressure recovery. A proposed

alternate method of boundary-layer control would use vortex generators to energize rather than remove the inlet throat boundary layer. If successful, the advantages of reducing or eliminating the bleed flow would be to decrease inlet drag and to decrease inlet size. For proper operation, these vortex generators must be placed forward of the point requiring boundary-layer control. Thus to control the inlet throat boundary layer the generators must be located in the supersonic portion of the inlet.

Most of the past experimental tests with vortex generators have been conducted at subsonic speeds. Reference 1, however, reports results obtained with vortex generators operating in both subsonic and supersonic flow. In that investigation vortex generators were installed immediately downstream of the inlet throat on the centerbody of an axisymmetric inlet. The generators increased diffuser pressure recovery and reduced distortion by injecting high-energy air into the normally retarded flow region adjacent to the centerbody. This boundary-layer control continued during supercritical inlet operating with the generators operating upstream of the inlet terminal shock in supersonic flow. References 2 and 3 also report the ability of vortex generators to control boundary-layer and shock interaction while operating in supersonic flow.

An experimental test program was conducted in the Lewis 10- by 10-Foot Supersonic Wind Tunnel to determine the performance of vortex generators placed in supersonic flow forward of the throat of a mixed-compression inlet. The Mach 2.5, 40-percent-internal-contraction inlet of reference 4 was chosen as the test vehicle. Three vortex generator locations within the inlet were selected for study: (1) a forward centerbody location to control the interaction of the cowl-lip-generated oblique shock and the centerbody boundary layer; (2) an aft centerbody location to control the terminal-shock and centerbody-boundary-layer interaction; and (3) a cowl location to control the terminal-shock and cowl-boundary-layer interaction.

The performance of the vortex generators, in terms of energizing the boundary layer and improving the inlet pressure recovery, was determined initially without inlet throat bleed and finally in combination with throat bleed. The test was conducted at Mach 2.5 and a Reynolds number of 3.88×10^6 based on inlet cowl lip diameter.

SYMBOLS

AR	aspect ratio
c	airfoil chord, cm
h	vortex-generator height, cm
M	Mach number
m/m_0	mass-flow ratio

P total pressure, N/m^2

S spacing between sets of divergent vortex-generator pairs, cm

s spacing between airfoils of a converging or diverging vortex-generator pair, cm

t maximum airfoil thickness, cm

δ boundary-layer height, cm

θ_l cowl-lip-position parameter, $\tan^{-1} 1/(x/R)$

Subscripts:

by bypass

con converging vortex generators

div diverging vortex generators

l local

max maximum

min minimum

0 free stream

5 diffuser exit station

Superscript:

— average

APPARATUS AND PROCEDURE

Inlet Model

The inlet used in this investigation was an axisymmetric mixed-compression type designed for Mach 2.5. At this speed, 60 percent of the supersonic flow area contraction was external and 40 percent was internal. The inlet was attached to a cylindrical nacelle 0.635 meter in diameter in which a J85-GE-13 engine or a coldpipe choked-exit plug assembly could be installed. For this study only the coldpipe was used. Complete details of the inlet design and performance are given in reference 4.

At the design Mach number of 2.5 and a free-stream temperature of 390 K, the inlet matched the J85-GE-13 engine corrected airflow requirement of 15.83 kilograms per second by supplying to the engine 88.6 percent of the capture mass flow at a total-pressure recovery of 0.90. This resulted in an inlet capture area of 0.1758 square meter. Of the remaining inlet flow, 6 to 7 percent was allotted for performance bleed,

4 percent for engine cooling air, and the rest for overboard bypass flow which could be varied for terminal shock position control.

The inlet featured a bicone centerbody which utilized half-angle cones of 10° and 18.5° to provide the external compression (fig. 1). In concept, the two-cone design would require that the contraction ratio be varied by collapsing the second cone. But to simplify the mechanical design of the test inlet, the contraction ratio was varied by translating the centerbody rather than by collapsing the second cone. The initial internal cowl angle was 5°. The internal oblique shock generated by the cowl lip was theoretically canceled at the centerbody impingement point by a turn of the surface. The remaining compression of the flow to a throat Mach number of 1.3 was isentropic and was distributed over a distance of 0.4 of the inlet capture radius or 0.0946 meter.

The subsonic diffuser consisted of an initial throat region 4 hydraulic radii in length with a 1° equivalent conical expansion followed by the main diffuser. The diffuser just downstream of the throat was mated to an existing subsonic diffuser (ref. 5). Because of differences in throat radii between the inlet of reference 5 and the inlet selected from reference 4 for this test, a relatively sharp curve in the cowl contour was required at the diffuser mating location. The overall design length, cone tip to compressor face, was 7.88 cowl lip radii.

The aft portion of the subsonic diffuser contained three hollow centerbody support struts which were used to duct the centerbody bleed flow overboard and which divided the duct into three compartments back to the engine face. The diffuser also included two bypass systems: a high-response overboard system for shock position control, and a low-speed valve to control secondary flow through the nacelle for engine cooling (fig. 1). The duct entrance into the bypass plenum contained louvered segments, as used in reference 4, to minimize plenum resonance.

Vortex Generators

The vortex generators selected for this test and placed in the supersonic portion of the inlet were designed by using information obtained mainly from reference 2. Both rectangular and triangular generators were tested in that investigation at Mach numbers as high as 1.35. Rectangular generators were selected for the present test. Rows of generators were placed within the inlet at the locations shown in figure 2. Placement of the generators conformed as closely as possible to a criterion of reference 2 which required that the generators be placed approximately 24 boundary-layer heights forward of the shock and boundary-layer interaction point for the best performance. Actual placements were as follows. The forward centerbody vortex generators were about 28 boundary-layer heights forward of the cowl oblique shock impingement point. The aft centerbody generators were about 20 boundary-layer heights forward of the inlet throat,

which is the location of the normal shock at critical inlet operation. The cowl vortex generators were located without knowing the cowl boundary-layer height in the region of interest. However, it is estimated that the cowl generators are in excess of 24 boundary-layer heights forward of the inlet terminal shock. Placement of the centerbody generators in the subsonic diffuser was identical to that of reference 4. The theoretical local Mach numbers at which the supersonic vortex generators of the present test operated ranged from 1.58 for the cowl generators to 2.00 for the forward centerbody generators (fig. 2).

Figure 3 shows the spacing of the vortex generators used at each of the locations shown in figure 2. All the generator configurations are listed in table I and all those having generators at 9° angle of attack are shown photographically in figure 4. Figure 5 presents the planform and cross section of the generators used at each inlet location and shows the relative size of each. All the spacings shown in figure 3 were measured from the generator midchord. For each configuration, the generators were arranged in diverging pairs with each generator set at the selected angle of attack and the flat surface facing upstream. This arrangement produced a system of counter-rotating vortices.

There were two spacing arrangements tested using the forward centerbody vortex generators. Configurations FCB-18 and FCB-9 used the first arrangement. This was the even spacing normally used with vortex generators (fig. 3(b)). In the second arrangement (configuration UFCB-18) the generators were spaced unevenly as shown in figure 3(c). To accomplish this, the spacing of adjacent diverging generators was reduced and the spacing of adjacent converging generators was increased. This arrangement theoretically increases the downstream range of effective vortex action (refs. 1, 6, and 7). In designing the generators, the spacing of all the vortex-generator configurations was related to the generator height h. The relative heights are shown in figure 5. For the evenly spaced configurations the spacing between adjacent generators s ratioed to the generator height h was maintained between 3.6 and 4.1. The exact spacing-to-height ratio for each configuration is given in table I.

Another variable tested using the forward centerbody generators was the generator angle of attack. Although reference 2 suggested 18° as an optimum angle (configuration FCB-18), a smaller angle of 9° was also investigated with configuration FCB-9. The lesser angle would reduce the strength of the vortices but would also reduce the airfoil drag (ref. 8). This angle variation was also tested using the aft centerbody generator configurations SACB-9 and SACB-18 (table I). The optimum angle of 16° used with the subsonic vortex generators in references 1 and 4 was unchanged.

Two sizes of generators were tested at the aft centerbody generator location. The spacing arrangement of the smaller configurations, SACB-9 and SACB-18, is shown in figure 3(d) and that of the larger configuration LACB-9 in figure 3(e). As these figures and table I indicate, the change in size was made without changing the generator spacing-to-height ratio. Based on information available primarily from references 2 and 3, the

vortex-generator height that might yield optimum performance was selected to be about 1.2 times the boundary-layer height. The larger height ratio of 2.4 used at the aft centerbody location would theoretically increase the downstream range of vortex action at some loss in overall effectiveness due to the increased height of the vortex from the surface. All the other configurations except the cowl vortex generators (configuration C-9) were the optimum height. The cowl boundary-layer height had not been previously determined and the cowl generators were made the same size as the forward centerbody generators (table I).

The cross-section and design details of each vortex generator used in the supersonic portion of the inlet are shown in figures 5(a) to (c). The three generators shown are identical except for size. The downstream surface of each generator was a three-straight-line approximation of the surface of an NACA 0012 airfoil. The upstream surface was the original airfoil mean-camber line (a straight line in this instance). This design approximated the vortex-generator cross section used in references 1 and 4. Generator thickness-to-chord ratio was 0.06. An aspect ratio of 1.0 was used for these supersonic generators as suggested by reference 2.

The subsonic generators used in the inlet diffuser were identical to those used in reference 4. The airfoil aspect ratio of 0.5, the thickness-to-chord ratio of 0.06, and the airfoil cross-section shape as shown in figure 5(d) were unchanged from the initial design in reference 1.

Instrumentation

Total-pressure rakes were positioned in the inlet to measure the performance of the variously placed vortex generators (fig. 6). Forward centerbody rakes were located to detect vortices produced by the forward centerbody vortex generators (fig. 6(a)). Similarly, cowl rakes were located to detect vortices from the cowl generators. The throat rakes would also be able to detect vortices, except those produced by the forward centerbody generators. Vortices from the forward centerbody generators would dissipate before reaching the throat rake location. As shown in figure 6(b) several rakes were installed at each axial rake position. The circumferential positions of each set of rakes were carefully chosen to eliminate mutual interference and, most importantly, to measure the pressures in the vortex fields aft of both diverging and converging generator pairs for all possible configurations.

Figure 7 shows the compressor-face pressure instrumentation (station 5). The overall diffuser total-pressure recovery was determined from rakes 1 to 6, which were area weighted. The additional measurement by rake 7 was included in the distortion calculations.

Inlet Bleed Configurations

The perforated bleed areas indicated in figure 1 were designed to control the inlet throat boundary layer, as reported in reference 4. The rows of holes comprising each bleed region are indicated schematically in figure 8(a). The basic bleed hole pattern of each of the bleed regions was obtained by staggering alternate rows of 0.3175-centimeter-diameter holes. This basic pattern is illustrated by the completely open cowl bleed pattern used in bleed configuration 1, as shown in figure 8(b). Bleed patterns were varied from this arrangement by filling selected bleed holes. The resulting three bleed configurations used in this investigation are shown in figure 8. Inlet performance resulting from the use of bleed configurations 2 and 3 is reported in reference 4.

The cowl bleed airflows were discharged overboard through the exits shown in figure 1. The exits had a 20° discharge angle relative to the external surface. Airflows from the centerbody bleed areas were discharged into a single plenum and then directed through the hollow centerbody support struts to 30° louvered exits. All exits were sized large enough to ensure choking of the bleed holes.

Test Procedure

Performance of vortex-generator configurations mounted at the forward centerbody location and at the aft centerbody location were first determined with no centerbody bleed (bleed configuration 1). During these tests and during testing of a control configuration, which used neither generators nor centerbody bleed, an excessive amount of cowl bleed was needed to ensure started inlet operation at the design centerbody position. Later tests determined the performance of the cowl and aft centerbody vortex generators in combination with the realistic bleed configurations 2 and 3. The centerbody vortex generators in the subsonic diffuser remained in place throughout these tests. These were finally removed when large supersonic vortex generators were tested at the aft centerbody position as an alternate method of diffuser boundary-layer control.

DISCUSSION OF RESULTS

Performance of Vortex Generators at Forward Centerbody Location with Bleed Configuration 1

Figures 9 to 11 present pitot-pressure boundary-layer profiles measured by the forward centerbody rakes. The profiles generated by the flow fields aft of the three forward

centerbody vortex-generator configurations are shown compared to the profiles measured without the generators installed. Each profile is labeled with the type of generator pair (converging or diverging) located upstream of the rake. The lateral position of each rake (relative to the vortex generators) is shown for each profile as a fraction of the distance between generators. For example, the fraction 1/2 would mean that the rake was positioned midway between two generators.

All the forward centerbody vortex-generator configurations produced active vortex flow fields (figs. 9 to 11). Each configuration injected high-energy air into the boundary layer aft of diverging generator pairs. Lower energy air was observed in the boundary layer aft of converging generator pairs. However, the boundary-layer degradation (or energy removal) aft of the converging pairs seemed greater than the energy injection aft of diverging pairs, especially for the evenly spaced configurations FCB-18 and FCB-9. The figures also show that a good boundary-layer profile existed aft of the cowl shock impingement point without boundary-layer control. Thus the generators were being required to energize a relatively good boundary layer which exhibited no adverse effects of the shock impingement.

The throat-exit-rake pressure profiles produced by all three forward centerbody vortex-generator configurations showed that each configuration degraded rather than energized the boundary layer. These data are presented in figures 12 to 14. Direct comparisons of the pitot profiles were meaningful at this location because the vortices had largely dissipated. Reference 1 reports that a distance of 8 generator pair spacings S was required for vortex dissipation. The distance from the forward centerbody generators to the throat exit rakes was 10.4S for the evenly spaced configurations. For configuration UFCB-18 the distance (based on a converging pair) was only 7S and some expected evidence of vortices still remained (fig. 14).

The inlet performance at peak recovery conditions for each of the three generator configurations is compared in figure 15 with the inlet performance without the vortex generators installed. The data are plotted against the cowl-lip-position parameter θ_l. All the generator configurations produced a loss in inlet total-pressure recovery, as expected after viewing figures 12 to 14. The configuration having the lowest generator angle of attack, FCB-9, the concomitantly the lowest drag (ref. 8), produced the smallest recovery loss - ranging from 0.005 to 0.010. The 18°-angle-of-attack configurations suffered 0.010 to 0.015 losses in recovery. The use of the forward centerbody generators also decreased the amount of internal inlet contraction permissible without causing unstart. This loss is illustrated in figure 15 by the reduction in the right limit of each vortex-generator curve. The trends generally follow the recovery loss trends. Without generators, inlet bleed configuration 1 allowed the centerbody to be retracted to a cowl-lip-position parameter θ_l of 25.49°. The 9°-angle-of-attack generators reduced this to a θ_l of 25.24°, and the uneven 18° generator configuration reduced the

attainable θ_l to 24.82°. The forward centerbody vortex-generator configurations had no significant effect on distortion.

Two factors may have contributed to the poor performance of the forward centerbody generators: (1) the relatively good boundary layer prior to the use of generators; and (2) the relatively high Mach number of 2.00 at the generator location. Reference 3 reports that increasing the supersonic Mach number lowered the generator performance.

Performance of Vortex Generators at Aft Centerbody Location with Bleed Configuration 1

Because the vortices from the forward centerbody vortex generators were largely dissipated before reaching the inlet throat, they could not control the terminal-shock and boundary-layer interaction. Vortex generators for this purpose were placed at the aft centerbody location. As the throat-rake pitot-pressure profiles of figures 16 and 17 show, all three aft generator configurations produced active vortices that persisted to the throat and through the terminal shock (fig. 17). (The distance from the generators to the throat exit rakes was well below the dissipation distance of 8S.) The aft centerbody generators were able to improve the boundary layer directly aft of the diverging generator pairs (figs. 16(a) and 17(a)). The boundary layer aft of the converging pairs was not in all cases as degraded as with the forward centerbody generators. The small aft generator configurations were pumping high-energy air, from aft of diverging pairs, along the vortex path and into the lower boundary layer aft of the converging generator pairs. Compare figure 9(c) with figures 16(b) and 17(b) and examine, for example, the pressures recorded by the probe next to the wall. The 18°-optimum-angle-of-attack generators (SACB-18) were more effective than the 9° generators (SACB-9) in pumping high-energy air into the lower boundary layer. This indicated that the 18° generators were, in this instance at least, producing the expected stronger vortex than the 9° generators. The large aft center body generators (LACB-18) were the least effective configuration in energizing the boundary layer.

The effects of these aft centerbody generator configurations on inlet performance at peak recovery conditions are presented in figure 18. Near the design contraction ratio (cowl-lip-position parameter θ_l of 25.28°), the use of generators having the optimum design height (h/δ of 1.2) had little effect on the inlet total-pressure recovery. The installation of larger generators (h/δ of 2.4), however, reduced the recovery by 0.015. This was somewhat anticipated in view of the boundary-layer data (figs. 16 and 17) and the results of reference 9, which reported that using one-half the number of double-height generators would cause a 50-percent increase in the generator system drag. At smaller inlet contraction ratios (θ_l less than 25°) the installation of the optimum-height

generators increased the inlet total-pressure recovery about 0.01. Also the recovery loss at design conditions resulting from the use of the larger generators was reduced by decreasing θ_l.

The vortices produced by the aft centerbody vortex-generator configurations also modified the inlet distortion levels. At a cowl-lip-position parameter θ_l of 25° and above, all the aft generator configurations increased distortion. At design θ_l, distortion was increased about 1 percent. Below a θ_l of 25°, however, all aft generator configurations decreased distortion. A maximum reduction of 1 percent occurred at the smallest θ_l. The amount of internal contraction allowable without causing inlet unstart was only slightly reduced (from a θ_l of 25.49° to 25.38°) by installing the aft centerbody generator configurations SACB-18 and LACB-9. The optimum-height, 9°-angle-of-attack generators did not change the allowable contraction.

Enlightenment on these performance trends was gained from a detailed examination of the throat-rake pitot-pressure profiles obtained with a more open inlet throat (or a smaller θ_l (fig. 19)). A close examination of figure 19 and comparison with figure 17 will reveal that the diverging generator pairs added more high-energy air to the boundary layer at the smaller θ_l than they did at the design θ_l. In addition, the boundary-layer degradation aft of converging generator pairs was less at the more open throat condition than at the design condition. Thus the recovery gain obtained by the smaller aft centerbody generators appear to be caused by an improvement of the local boundary layer by the generators at the more open inlet throat conditions.

This boundary-layer improvement was related to the effects of the terminal-shock and inlet-boundary-layer interaction. An empirical determination in reference 10, at test conditions similar to those of the present test, revealed that a shock-induced static-pressure rise of about 1.9 was required to cause boundary-layer separation. This would mean that shock-induced separation could occur in the present test if the inlet terminal shock occurred at a Mach number above 1.33. Figure 20 compares the pressure recovery obtained with each aft centerbody generator configuration with the recovery obtained without generators. Data are presented as a function of the Mach number at the terminal shock location. In figure 20(a) the Mach number was varied by changing the inlet internal contraction ratio. In figure 20(b), supercritical inlet operation varied the Mach number. The trends in figure 20 are clear. The optimum-height vortex generators improved the inlet pressure recovery when the terminal shock occurred at or above a Mach number of about 1.34. It therefore seems evident that the optimum designed vortex generators improved local boundary layer when, and only when, the boundary layer was in incipient separation in the throat region. Under conditions in which the boundary layer was not tending to separate in the throat, the generators only degraded the boundary layer.

Performance of Cowl and Aft Centerbody Vortex Generators in Combination with Throat Bleed

For this portion of the test, the cowl and the small aft centerbody vortex generators were set at 9° angle of attack. These generator configurations were evaluated while using bleed configurations 2 and 3 (fig. 8). The performance of the inlet using these two bleed configurations is reported in reference 4. Both bleed systems utilized bleed on the forward cowl and forward centerbody. Bleed configuration 3 alone had aft cowl and aft centerbody bleed.

The performance of the cowl vortex generators, as measured by the cowl rakes, is presented in figure 21. These rakes were positioned just aft of the forward cowl bleed region (fig. 6). The term "alternate rake" referred to in figure 21 and in later figures identifies the rakes that were used on the inlet when bleed configurations 2 and 3 were installed without the supersonic vortex generators (ref. 4). These rakes were not the same rakes as were used when the inlet was tested with the generators installed. They were located at the same axial stations but at different circimferential positions. These dissimilarities, rake-to-rake variations in tap locations, and slight flow field asymmetry would then negate a comparison of minor rake-to-rake data variations as was made with figures 17 and 19.

The pitot-pressure profiles of figure 21 show that the cowl vortex generators produced almost no improvement in the boundary layer aft of the diverging generator pairs, but produced a large region of pressure deficiency aft of the converging pairs. The almost total lack of boundary-layer improvement aft of the diverging generators was unexpected. The aft centerbody generators of similar design, SACB-9, were operated at about the same local Mach number as the cowl generators (fig. 2) and were able to inject higher energy air into the boundary layer (fig. 17). However, some degradation from the performance of the aft centerbody generators was expected with the cowl generators because their height ratio h/δ was most certainly larger than the optimum value of 1.2 used for configuration SACB-9. The data of figure 21 can be explained if the porous cowl bleed region just aft of the generators was affecting the vortices produced by the cowl generators. With bleed configuration 2, this region removed 0.022 of the inlet capture mass flow; bleed configuration 3 removed 0.015 of the capture mass flow. The affected vortices persisted unchanged from the cowl rakes (fig. 21) to the throat rakes (see the upper part of fig. 22(a)) and were unchanged in crossing the normal shock (fig. 22(b)). These vortices were also unchanged in passing over the aft cowl bleed of bleed configuration 3. This is revealed by comparing figure 23 with figure 22 and noting that the cowl-side throat-exit pressure profiles are similar. Two conditions may explain why this bleed did not affect the vortices as did the forward cowl bleed. First, the aft bleed was much farther downstream of the generators than the forward cowl bleed and therefore was

not subjected to the same initial, and probably most intense, vortex flow field. Second, the amount of aft cowl bleed was smaller than the amounts of forward cowl bleed (the aft cowl bleed being $0.008 m/m_0$ at peak conditions).

The location of the aft centerbody vortex generators relative to the bleed areas of bleed configurations 2 and 3 can be seen by referring to figures 2 and 8. Unlike conditions on the cowl (where the first bleed region was located aft of the generators) the forward bleed region on the centerbody was ahead of the aft centerbody generators. Although the amount of forward centerbody bleed was small, being about $0.004 m/m_0$, it would reduce somewhat the boundary-layer height encountered by the aft centerbody generators. Some degradation in vortex generator performance might therefore be expected due to the resulting nonoptimum height ratio h/δ. However, the data indicate that the vortex action was not significantly changed by bleeding in front of the generators. This seemed evident because the vortices produced by the aft centerbody generators and forward bleed combination (as reflected by fig. 22) were similar to those generated by the aft centerbody generators without the forward centerbody bleed (figs. 16 and 17).

Bleed aft of the centerbody vortex generators was provided only by bleed configuration 3. This bleed region was much farther aft of the aft centerbody generators than the forward cowl bleed region was aft of the cowl generators (fig. 2). This is believed to be a significant factor in the bleed results to follow. With the inlet at supercritical conditions, the aft centerbody bleed of configuration 3 removed $0.016 m/m_0$. This amount of bleed was nearly the same as the amount removed by the forward cowl bleed, but it did not affect the vortex action produced by the aft centerbody generators as greatly as it affected the vortex action produced by the cowl generators. On the centerbody, the boundary-layer energy addition aft of the diverging generator pairs and the boundary-layer degradation aft of the converging generator pairs was of the same general magnitude with and without the aft centerbody bleed (compare figs. 22(a) and 23(a)). At peak inlet conditions, the aft centerbody bleed removed a larger amount of flow ($0.032 m/m_0$). This amount of bleed had a greater effect on the vortex action produced by the aft centerbody generators. The result was that little high-energy flow was added to the uniform flow field aft of the diverging generator pairs. (Compare the 1/4-diverging curve in fig. 23(b) with the alternate-rake curve.) Compare this result with the greater energy addition aft of the diverging generators without the aft bleed (fig. 22(b)). Aft of the converging generator pairs, the uniform flow was degraded more by the generators and the 0.032-mass-flow-ratio bleed combination (i.e., configuration 3) than by the generators alone (configuration 2).

It thus seems that when the vortex generators were located immediately upstream of a porous bleed region having about 0.020 mass-flow ratio removed (as with the cowl generators), the vortex flow field was significantly degraded by the bleed. When the generators were located at a more upstream position relative to the bleed region, as with the aft centerbody bleed and generators, larger amounts of bleed flow removal (0.032 mass-

flow ratio) were sustained before the vortex flow field was significantly degraded.

A tentative explanation for the boundary-layer degradation observed when bleed was placed aft of vortex generators is that there was selective bleeding of the nonuniform flow field. It is possible that the porous bleed areas removed primarily higher energy flow from the lobes of the vortices as they approached the bleed surface and then injected some of the low-energy air from the bleed plenum back into the external flow field at points where the vortices were directing flow away from the surface. In this hypothetical picture, there is an increase in the local surface static pressure just aft of diverging generator pairs (where the higher energy lobes approach the surface) and a decrease in the surface static pressure just aft of converging generator pairs (where the vortices direct flow away from the surface). The degrading effects of bleeding in the vortex flow field might then be avoided by using a nonuniform bleed that was tailored to selectively remove only the lower energy air aft of the converging generator pairs.

The performance of the inlet with cowl and aft centerbody vortex generators in combination with bleed configurations 2 and 3 is presented in figures 24 and 25, and compared with inlet performance with the bleed alone. Part (a) of each figure presents the performance at peak total-pressure recovery conditions, and part (b) presents the performance at the design cowl-lip-position parameter. When the generator configurations were installed in the inlet with bleed configuration 2, the peak total-pressure recovery was reduced by 0.01 to 0.02 over the tested range of cowl-lip-position parameter θ_l (fig. 24(a)). At the design θ_l, the peak recovery loss was 0.02 (fig. 24(b)). When the generators were installed in the inlet with bleed configuration 3, the peak pressure recovery obtained over the θ_l range was reduced by 0.02 to 0.035 (fig. 25(a)). The recovery loss at design θ_l was 0.025 (fig. 25(b)). By referring to figures 15 and 18 and comparing them to figures 24(a) and 25(a), it becomes apparent that none of the generator configurations tested with or without bleed could provide a peak inlet total-pressure recovery to match that obtained with a good throat bleed configuration.

The distortion curves in the upper portions of figures 24(a) and 25(a) show that the effect of adding vortex generators to the inlet with bleed configuration 2 or 3 was relatively constant over the tested θ_l range. A comparison of the absolute values of distortion in figures 24(a) and 25(a), between the configurations with generators and the configurations without generators, would not be valid because the data obtained without generators were also obtained without bypass flow whereas the data obtained with generators were obtained with bypass flow. Bypass flow in the amount used ($0.032 m/m_0$) significantly lowered distortion by controlling the boundary layer on the cowl side of the diffuser. Better distortion comparisons were available at the design θ_l condition (figs. 24(b) and 25(b)). The bypass flow variations shown on these figures did not noticeably affect distortion levels. The addition of the generators to the inlet with bleed configuration 2 increased the distortion at peak recovery conditions by 0.02. With bleed configu-

ration 3 used in the inlet, installation of the generators increased distortion at peak by 0.01.

At most supercritical inlet conditions above a total-pressure recovery of about 0.83, the installation of vortex generators in the inlet with either bleed configuration 1 or 2 substantially increased distortion (figs. 24(b) and 25(b)). Without these "supersonic" vortex generators (i.e., the cowl and aft centerbody generators), the distortion was low in this supercritical range because the subsonic-diffuser vortex generators located on the centerbody (fig. 2) were controlling the diffuser centerbody boundary layer. When the "supersonic" generators were installed in the inlet, the vortices from the aft centerbody generators trailed aft to the subsonic-diffuser vortex-generator station. According to the vortex dissipation criteria of reference 1, the vortices produced by the aft centerbody generators would still be active at the diffuser generator station. The resulting interference with the diffuser boundary-layer control produced the distortion increase noted. In fact, the resulting curves are similar to those reported in reference 4 where subsonic-diffuser generators were not used.

Below a total-pressure recovery of about 0.83, the inlet configurations without the "supersonic" vortex generators displayed a rapid rise in distortion (figs. 24(b) and 25(b)). These distortion curves are typical of those in reference 4 obtained with diffuser vortex generators employed as a centerbody boundary-layer control. The distortion rise resulted from the change in terminal shock location relative to the subsonic-diffuser vortex generators. At the beginning of the rise, the terminal shock passed aft of the diffuser generator station and the generators remained effective in controlling the shock and boundary-layer interaction. As the shock continued aft the generators continued to energize the retarded flow adjacent to the centerbody wall (but only when undisturbed by vortex flow from the "supersonic generators"). The better flow hugged the centerbody side of the duct and the flow on the cowl side tended to separate. This is opposite to results without centerbody generators in the diffuser or to results with "supersonic generators" forward of the centerbody diffuser generators. In these cases the best flow was near the cowl side and the flow on the centerbody side tended toward separation. This flow redistribution by the centerbody diffuser generators increased the distortion. Figure 26 shows this redistribution for an inlet configuration which used the diffuser vortex generators alone with bleed configuration 1. The ease with which the cowl-side flow tended to separate may have been caused by the relatively sharp curve in the cowl contour at the diffuser mating location. However, as already noted, no cowl-side separation occurred when the centerbody diffuser generators were not installed (fig. 26) or when the "supersonic generators" were forward of the diffuser generators.

Large Aft Centerbody Vortex Generators as a Diffuser Boundary-Layer Control

As has just been discussed, vortex generators located in the inlet subsonic diffuser were capable of energizing the diffuser boundary layer. This result was also reported in reference 1 where the use of diffuser generators increased total-pressure recovery and decreased distortion. A more forward location for generators intended to control the diffuser boundary layer might be more efficient because the terminal shock would always be downstream of the generator station. Accordingly, the large aft centerbody generators, LACB-9, were installed in the inlet and the diffuser generators were removed. The large generators were chosen because they would theoretically have a longer downstream range of effectiveness than the smaller generators. The results are shown in figure 26. The large generators at the aft centerbody position did not effectively energize the diffuser boundary layer. The cause of this failure may be, in part, that, based on the eight-pair spacing dissipation criterion of reference 1, the vortices produced by configuration LACB-9 dissipated midway through the subsonic diffuser whereas the vortices produced by the subsonic-diffuser vortex generators remained active over almost the whole diffuser length.

SUMMARY OF RESULTS

Vortex generators were installed in the supersonic portion of a mixed-compression inlet and studied as a means of throat boundary-layer control. Generators were placed at a forward centerbody location ahead of the cowl shock impingement point, at an aft centerbody location ahead of the inlet throat, and on the cowl at a location ahead of the throat. Performance of the centerbody generators was determined without centerbody bleed. The performance of cowl and aft centerbody generators in combination with inlet throat bleed was also determined. The test was conducted in the Lewis 10- by 10-Foot Supersonic Wind Tunnel at a free-stream Mach number of 2.5 with the following results:

1. With or without bleed, the "supersonic" vortex generators were unable to produce inlet peak recovery levels as high as available with a good boundary-layer bleed system.

2. Placement of vortex generators at a forward centerbody location to control the unbled-boundary-layer and cowl-shock interaction resulted in degradation of the boundary layer, a concomitant loss of about 1 percent in compressor-face total-pressure recovery, and a decrease in the attainable inlet contraction ratio.

3. Placement of vortex generators at a more aft centerbody position, to control the unbled-boundary-layer and terminal-shock interaction, reduced distortion and increased

total-pressure recovery about 1 percent each, but only at the more open inlet throat conditions. These performance gains resulted from an improved boundary layer produced by the vortex generators. This improvement by vortex generators was limited to conditions where the inlet terminal shock was capable of causing separation of the turbulent boundary layer.

4. Cowl and aft centerbody vortex generators in combination with selected inlet bleed configurations reduced by 1 to 3.5 percent the inlet total-pressure recovery attainable with bleed alone. Distortion at peak recovery conditions was increased 1 to 2 percent.

5. Locating bleed regions immediately downstream of vortex generators significantly degraded the vortex flow field.

6. The large aft centerbody vortex generators mounted forward of the inlet throat were unable to control the subsonic-diffuser boundary layer as effectively as do the generators mounted aft of the throat in the subsonic diffuser.

Lewis Research Center,
National Aeronautics and Space Administration,
Cleveland, Ohio, July 20, 1971,
764-74.

REFERENCES

1. Mitchell, Glenn A.; and Davis, Ronald W.: Performance of Centerbody Vortex Generators in an Axisymmetric Mixed-Compression Inlet at Mach Numbers From 2.0 to 3.0. NASA TN D-4675, 1968.

2. Powers, W. E.: Application of Vortex Generators for Boundary Layer Control Through a Shock. Rep. R-95477-6, United Aircraft Corp., July 11, 1952.

3. Karanian, A. J.: Characteristics of Normal Shock Waves in the Throats of Precompression Inlets. Rep. R-0955-20, United Aircraft Corp., Oct. 1957.

4. Wasserbauer, Joseph F.; and Choby, David A.: Mach 2.5 Performance of a Bicone Inlet with Internal Distributed Compression and 40-Percent Internal Contraction. NASA TM X-2416, 1972.

5. Cubbison, Robert W.; Meleason, Edward T.; and Johnson, David F.: Effect of Porous Bleed in a High-Performance Axisymmetric, Mixed-Compression Inlet at Mach 2.50. NASA TM X-1692, 1968.

6. Jones, J. P.: The Calculation of the Paths of Vortices From a System of Vortex Generators, and a Comparison With Experiment. Rep. C. P. 361, Aeronautical Research Council, Great Britain, 1957.

7. Pearcey, H. H.: Shock Induced Separation and Its Prevention by Design and Boundary Layer Control. Boundary Layer and Flow Control. Vol. 2. Gustav V. Lachmann, ed., Pergamon Press, 1961, p. 1166.

8. Cramer, R. H.: Mixing Devices for Delaying Separation. Research and Development Programs. Rep. U-RQR-67-1, Applied Physics Lab., Johns Hopkins Univ. (NASA CR-87061), Mar. 1967.

9. Whitten, J. J.: The Drag of Vane-Type Vortex Generators in Compressible Turbulent Flow. Rep. DRL-556, Defense Research Lab., Univ. Texas, Aug. 1967.

10. Nussdorfer, T. J.: Some Observations of Shock-Induced Turbulent Separation on Supersonic Diffusers. NACA RM E51L26, 1954.

TABLE I. - VORTEX-GENERATOR CONFIGURATIONS

Description	Generator angle of attack, deg	Configuration code	Vortex generator height, h, cm	Ratio of convergent spacing to height, S_{con}/h	Ratio of divergent spacing to height, S_{div}/h	Ratio of pair spacing to height, S/h	Spacing ratio, S/s_{div}	Design height ratio, h/δ	Number of generators
Forward centerbody vortex generators	18	FCB-18	0.444	3.66	3.66	7.32	2	1.2	56
	9	FCB-9	.444	3.66	3.66	7.32	2		
Forward centerbody vortex generators with uneven spacing	18	UFCB-18	.444	5.49	1.83	7.32	4		
Small aft centerbody vortex generators	9	SACB-9	.508	4.08	4.08	8.16	2		
	18	SACB-18	.508	4.08	4.08	8.16			
Large aft centerbody vortex generators	9	LACB-9	1.016	4.08	4.08	8.16		2.4	28
Cowl vortex generators	9	C-9	.444	3.94	3.94	7.88		---	88
Subsonic-diffuser centerbody vortex generators (ref. 4)	16	DIF	1.270	3.64	3.64	7.28		---	24

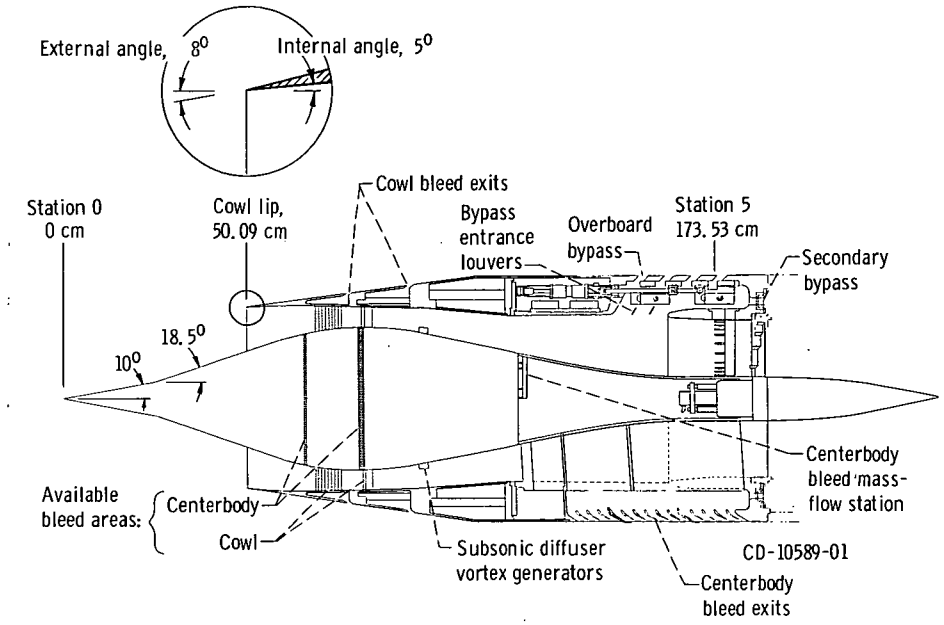

Figure 1. - Cross section of axisymmetric Mach 2.5 mixed-compression inlet.

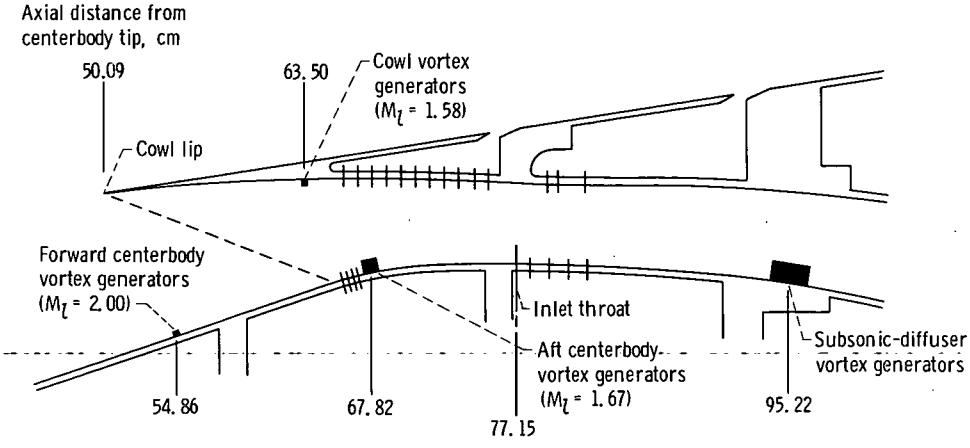

Figure 2. - Vortex-generator locations.

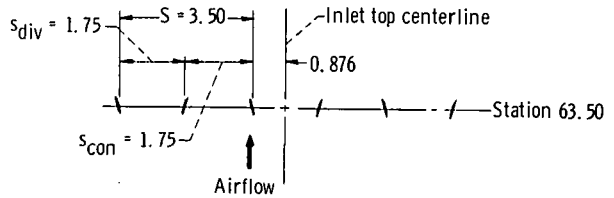

(a) Cowl vortex generators.

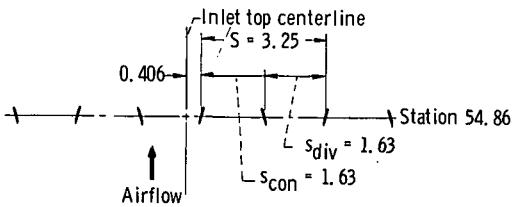

(b) Forward centerbody vortex generators.

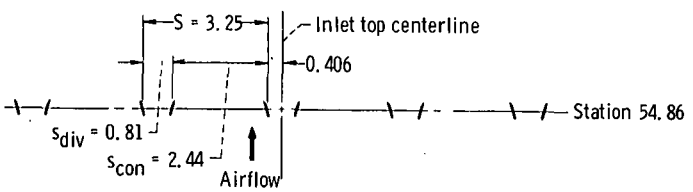

(c) Unevenly spaced forward centerbody vortex generators.

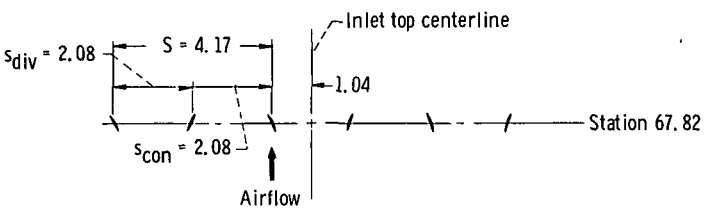

(d) Small aft centerbody vortex generators.

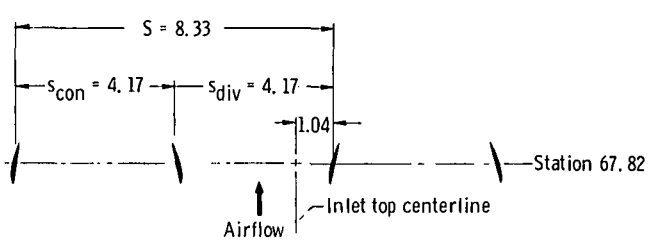

(e) Large aft centerbody vortex generators.

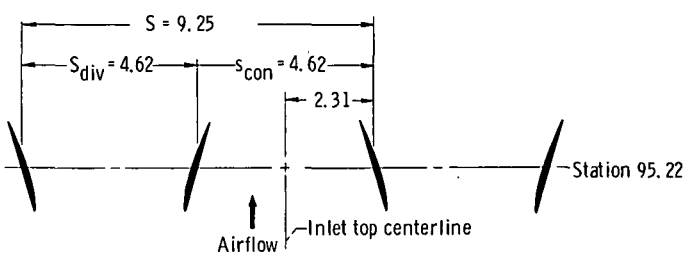

(f) Subsonic-diffuser vortex generators (ref. 4.)

Figure 3. - Vortex-generator spacing arrangements. (All dimensions are in centimeters.)

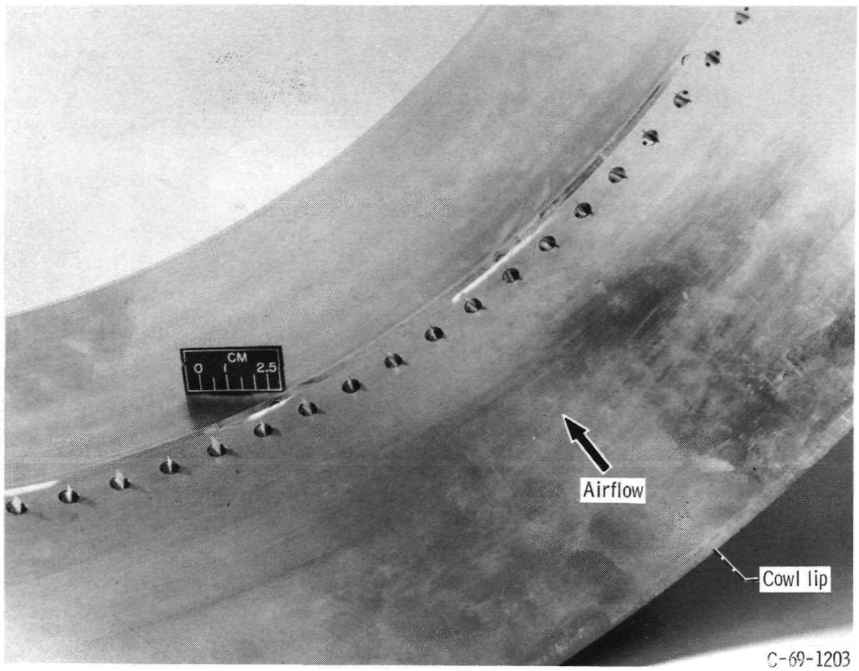

(a) Cowl vortex generators. Configuration C-9.

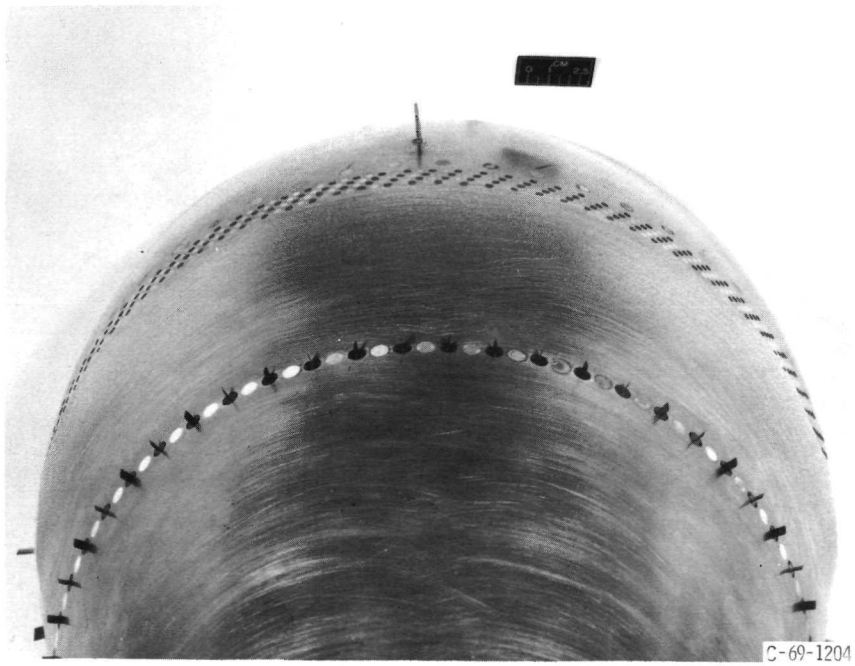

(b) Forward centerbody vortex generators. Configuration FCB-9.

Figure 4. - Installed vortex generators.

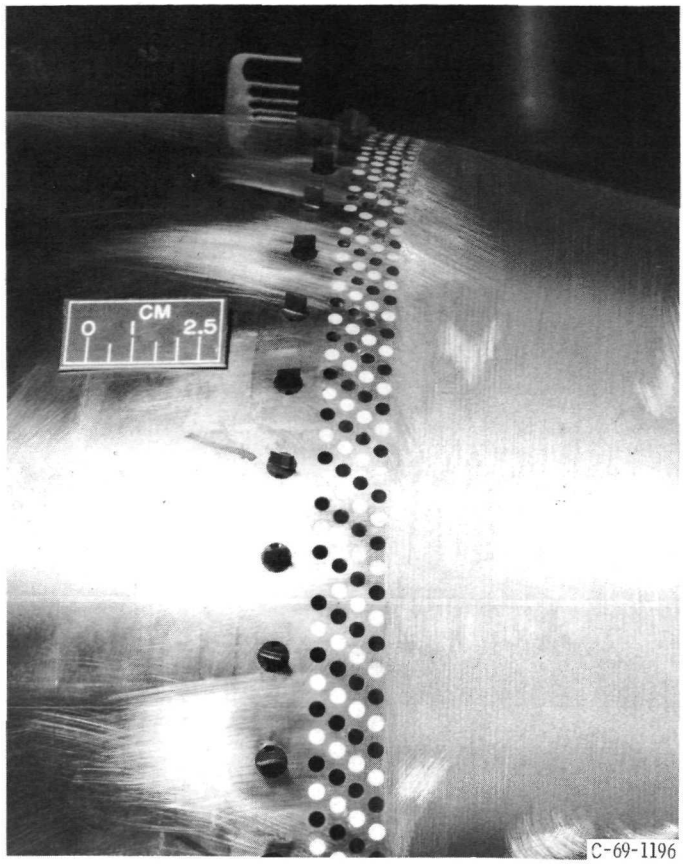

(c) Small aft centerbody vortex generators. Configuration SACB-9.

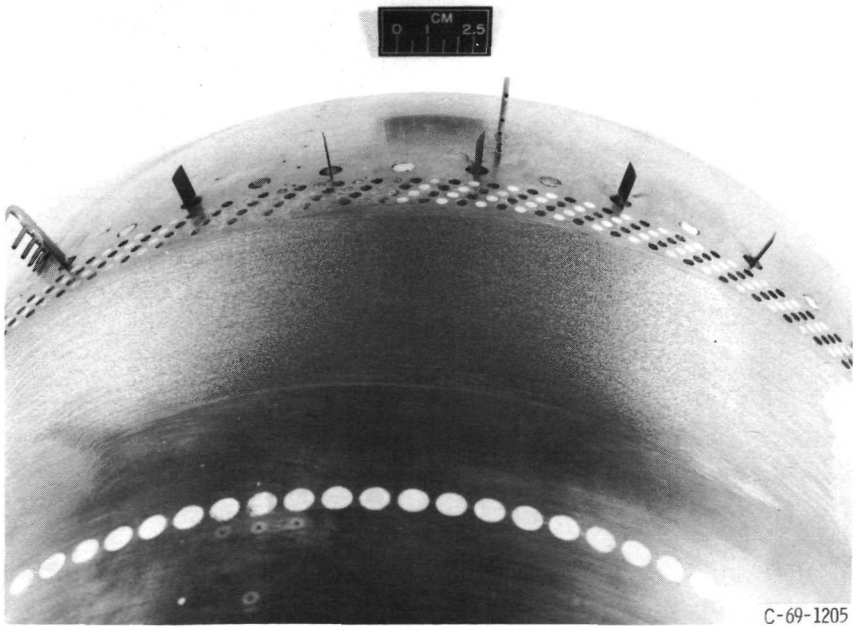

(d) Large aft centerbody vortex generators. Configuration LACB-9.

Figure 4. - Concluded.

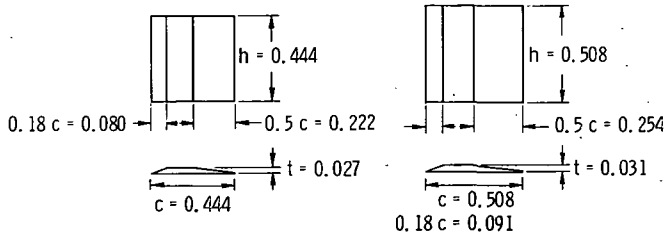

(a) Cowl and forward centerbody vortex generators. Aspect ratio, AR = 1.0; thickness-to-chord ratio, t/c = 0.06.

(b) Small aft centerbody vortex generators. AR = 1.0; t/c = 0.06.

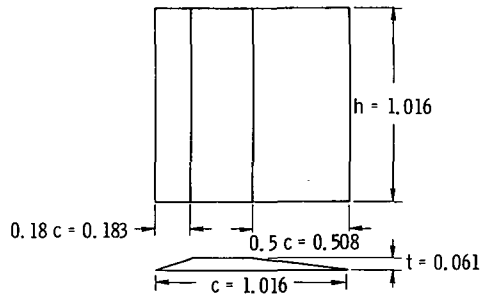

(c) Large aft centerbody vortex generators. AR = 1.0; t/c = 0.06.

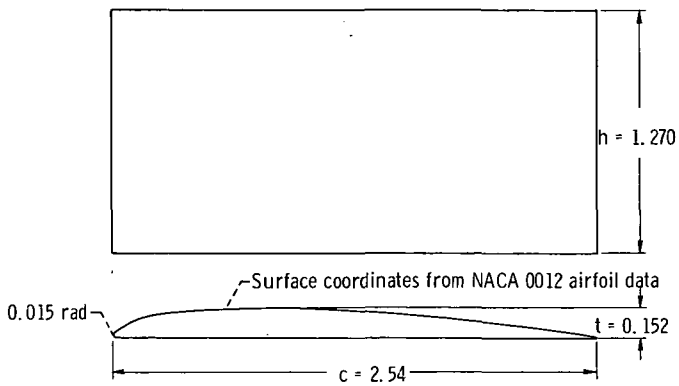

(d) Subsonic-diffuser vortex generators. AR = 0.5; t/c = 0.06. (Ref. 4.)

Figure 5. - Vortex-generator designs. (All dimensions are in centimeters.)

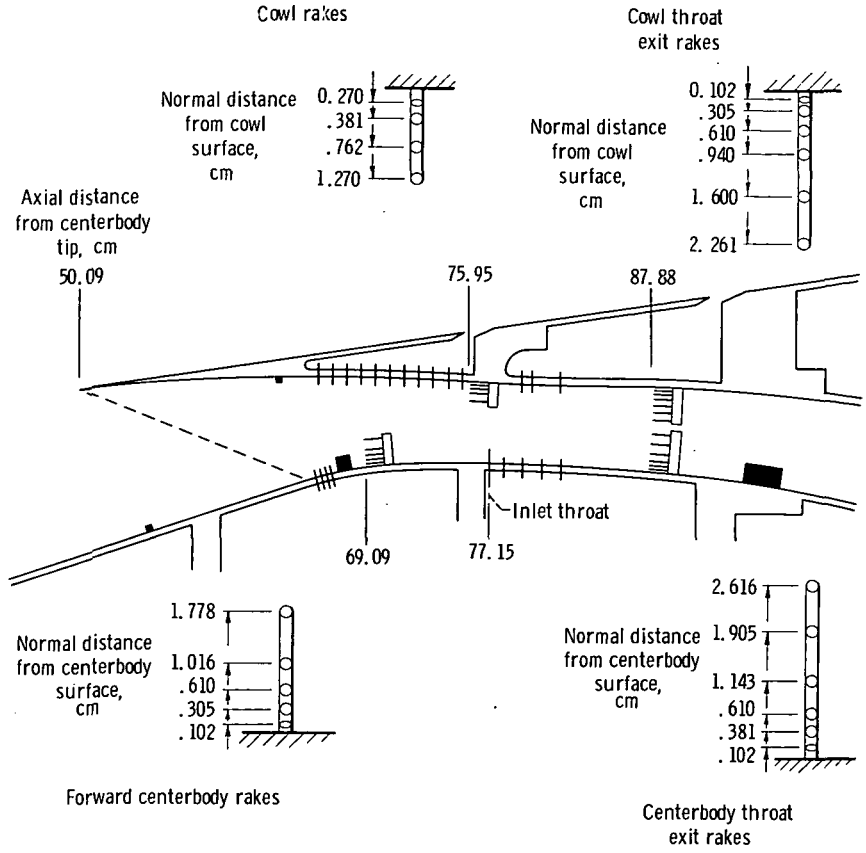

(a) Axial location of rakes, and probe to surface placements.

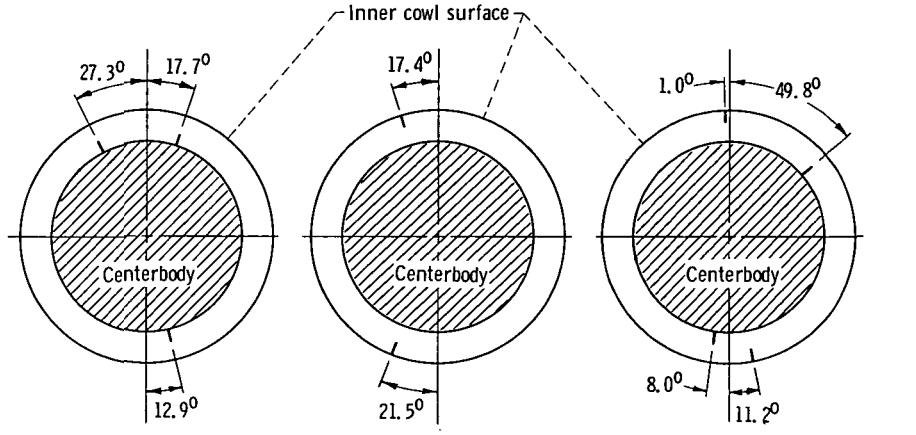

Forward centerbody rakes, 69.09 centimeters from centerbody tip

Cowl rakes, 75.95 centimeters from centerbody tip

Throat exit rakes, 87.88 centimeters from centerbody tip

(b) Circumferential location of rakes, looking downstream.

Figure 6. - Inlet rake instrumentation.

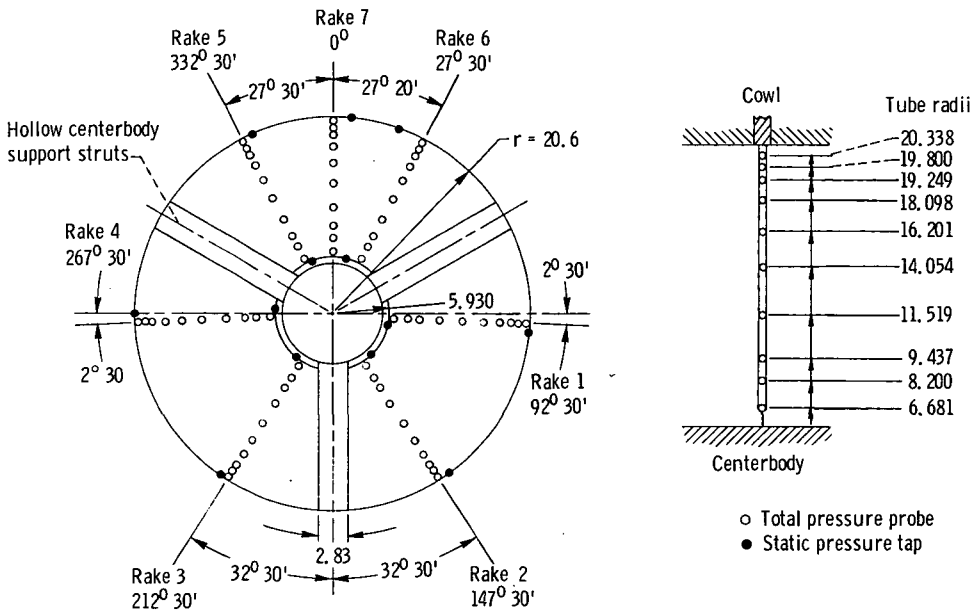

Figure 7. - Compressor face (station 5) instrumentation, looking downstream.
(all dimensions are in centimeters, unless noted.)

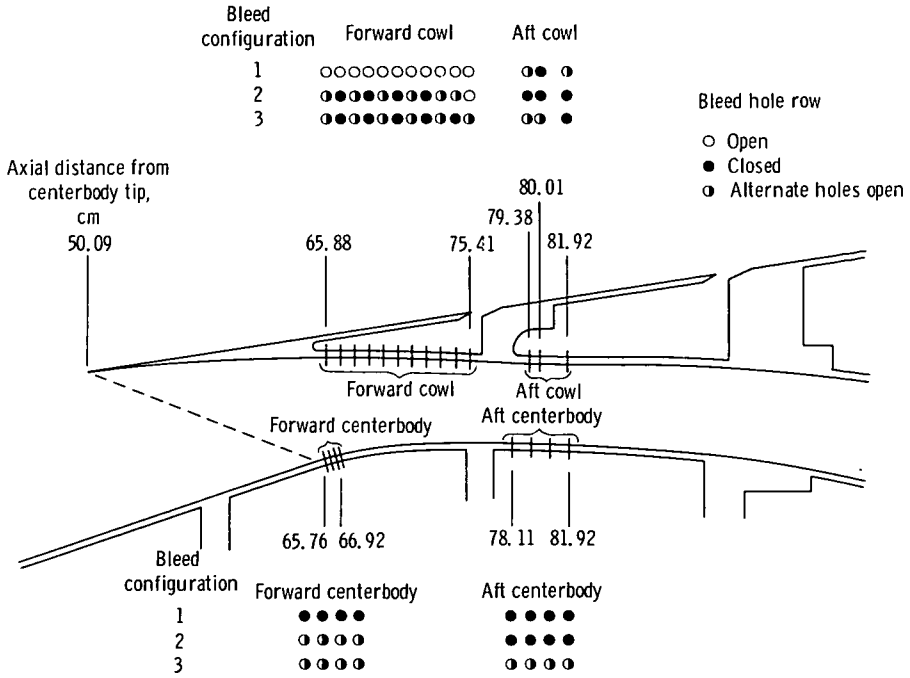

(a) Bleed locations.

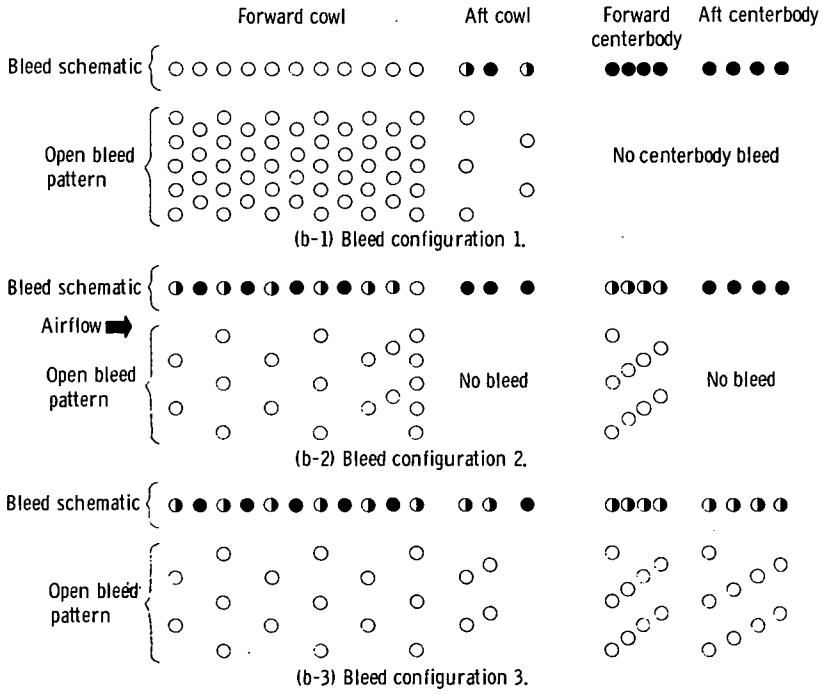

(b) Bleed patterns.

Figure 8. - Inlet bleed configurations. Bleed hole diameter, 0.3175 centimeter.

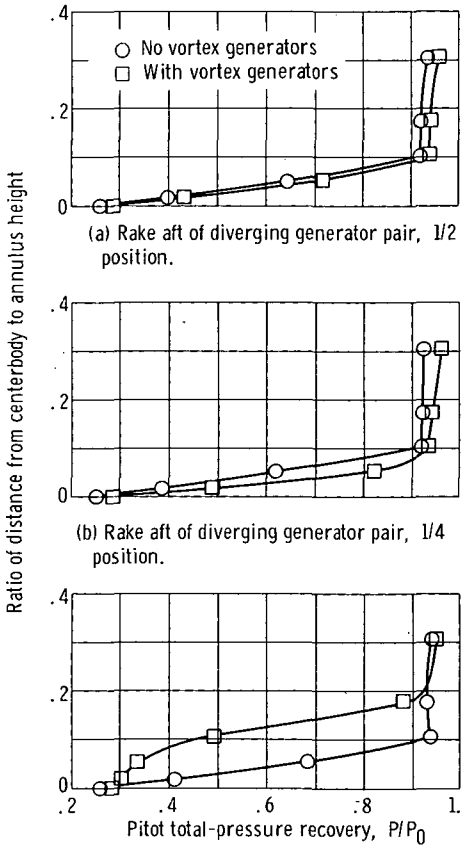

(a) Rake aft of diverging generator pair, 1/2 position.

(b) Rake aft of diverging generator pair, 1/4 position.

(c) Rake aft of converging generator pair, 1/2 position.

Figure 9. - Performance of forward centerbody vortex-generator configuration FCB-18 as measured by forward centerbody rakes. Cowl-lip-position parameter θ_l of 25.02°; bleed configuration 1.

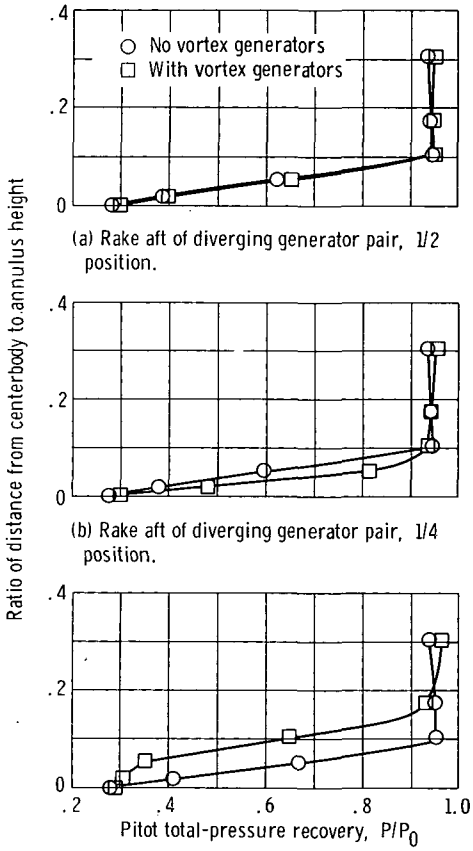

(a) Rake aft of diverging generator pair, 1/2 position.

(b) Rake aft of diverging generator pair, 1/4 position.

(c) Rake aft of converging generator pair, 1/2 position.

Figure 10. -Performance of forward centerbody vortex-generator configuration FCB-9 as measured by forward centerbody rakes. Cowl-lip-position parameter θ_l of 25.24°; bleed configuration 1.

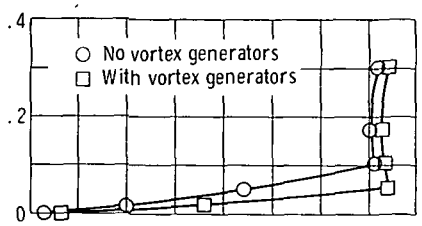

(a) Rake aft of divering generator pair, 1/2 position.

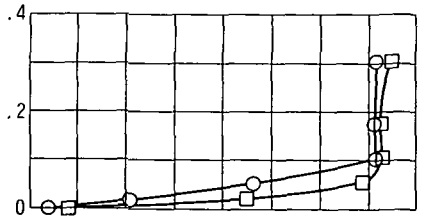

(b) Rake aft of generator centerline.

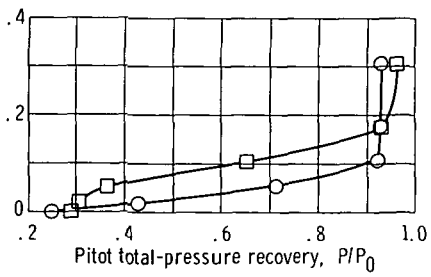

(c) Rake aft of converging generator pair, 1/3 position.

Figure 11. - Performance of forward centerbody vortex-generator configuration UFCB-18 as measured by forward centerbody rakes. Cowl-lip-position parameter θ_ℓ of 24.82°; bleed configuration 1.

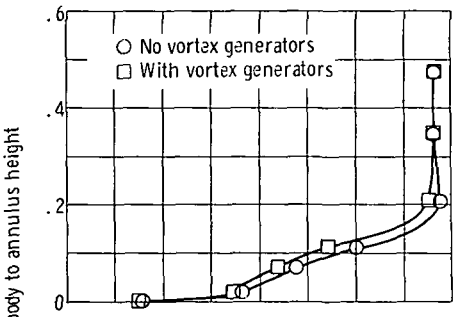

(a) Rake aft of diverging generator pair, 1/2 position.

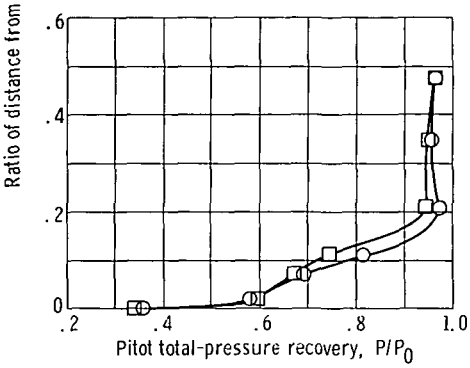

(b) Rake aft of generator centerline.

Figure 12. - Performance of forward centerbody vortex-generator configuration FCB-18 as measured by throat exit rakes, at supercritical inlet conditions. Cowl-lip-position parameter θ_ℓ of 25.02°; bleed configuration 1.

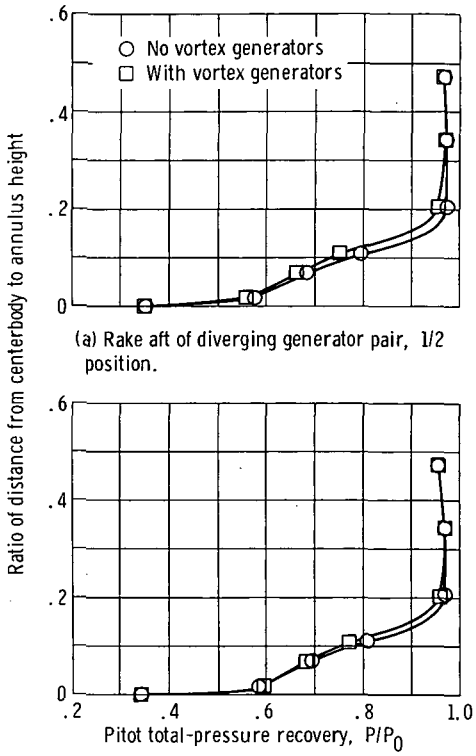

(a) Rake aft of diverging generator pair, 1/2 position.

(b) Rake aft of generator centerline.

Figure 13. - Performance of forward centerbody vortex-generator configuration FCB-9 as measured by throat exit rakes, at supercritical inlet conditions. Cowl-lip-position parameter θ_ℓ of 25.24°; bleed configuration 1.

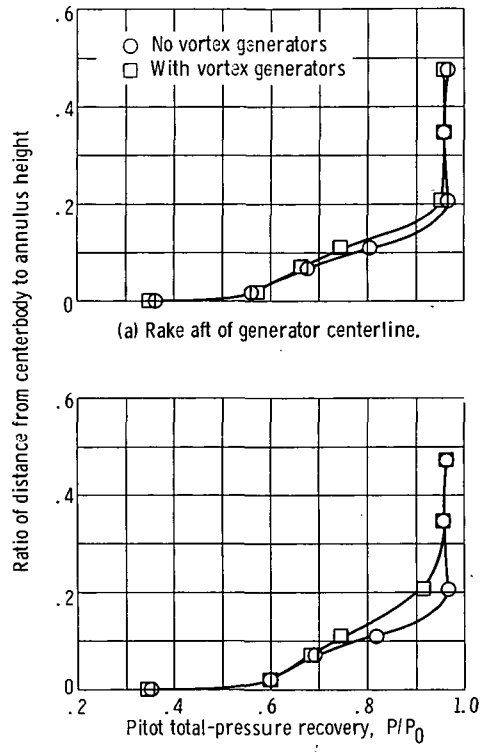

(a) Rake aft of generator centerline.

(b) Rake aft of converging generator pair, 1/3 position.

Figure 14. - Performance of forward centerbody vortex-generator configuration UFCB-18 as measured by throat exit rakes, at supercritical inlet conditions. Cowl-lip-position parameter θ_ℓ of 24.82°; bleed configuration 1.

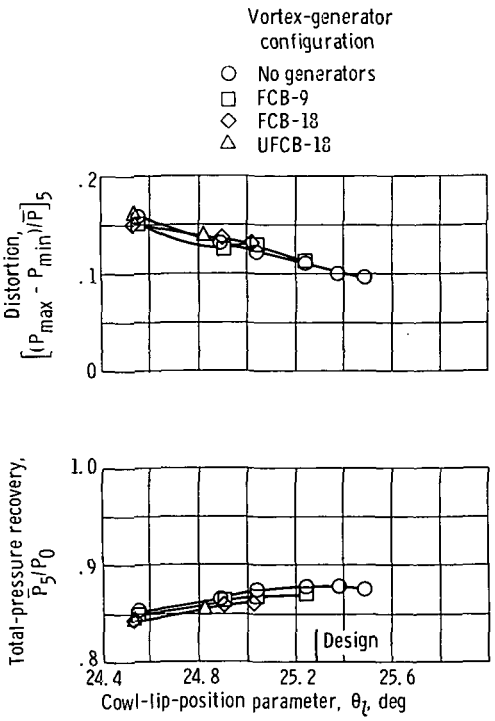

Figure 15. - Effect of forward centerbody vortex-generator configurations on inlet performance at peak recovery conditions. Bypass mass-flow ratio m_{by}/m_0 of 0.032; bleed configuration 1.

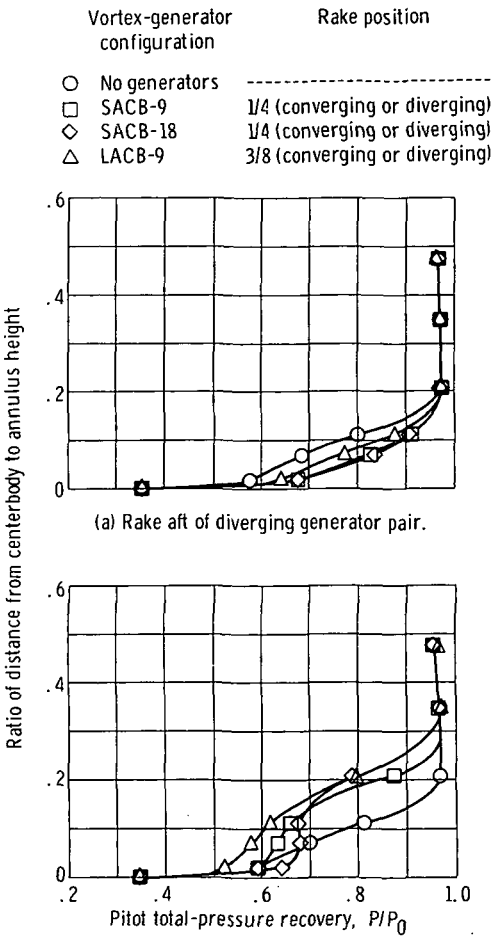

(a) Rake aft of diverging generator pair.

(b) Rake aft of converging generator pair.

Figure 16. - Performance of aft centerbody vortex-generator configurations at supercritical inlet conditions, as measured by throat exit rakes. Cowl-lip-position parameter θ_l of 25.26°; bleed configuration 1.

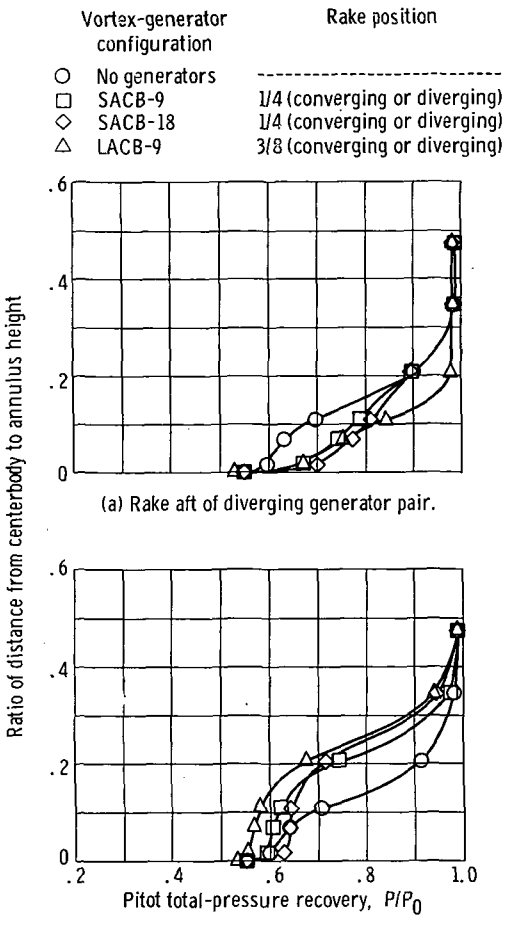

(a) Rake aft of diverging generator pair.

(b) Rake aft of converging generator pair.

Figure 17. - Performance of aft centerbody vortex-generator configurations at peak recovery conditions, as measured by throat exit rakes. Cowl-lip-position parameter θ_l of 25.26°; bleed configuration 1.

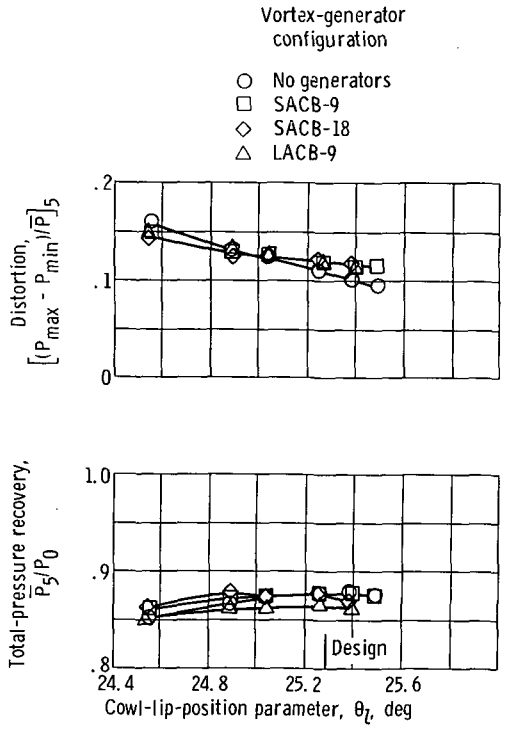

Figure 18. - Effect of aft centerbody vortex generators on inlet performance at peak recovery conditions. Bypass mass-flow ratio m_{by}/m_0 of 0.032; bleed configuration 1.

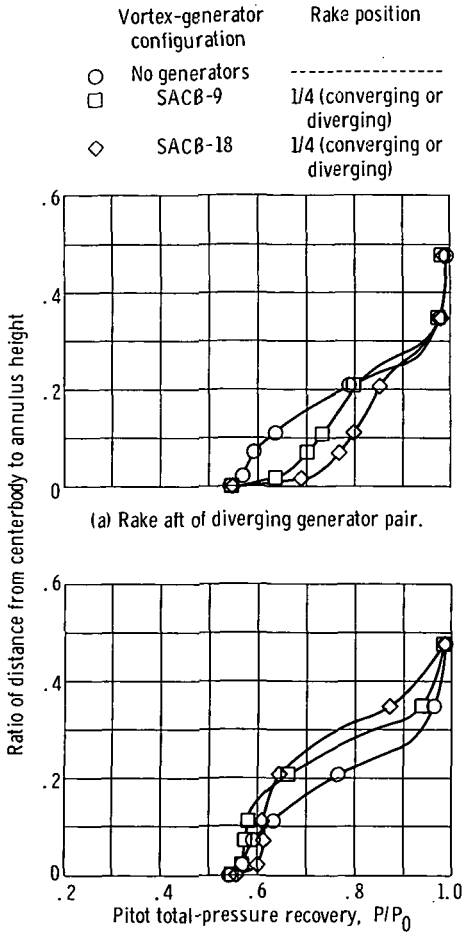

(a) Rake aft of diverging generator pair.

(b) Rake aft of converging generator pair.

Figure 19. - Performance of aft centerbody vortex-generator configurations at peak recovery conditions, as measured by throat exit rakes. Cowl-lip-position parameter, θ_ℓ of 24.54°; bleed configuration 1.

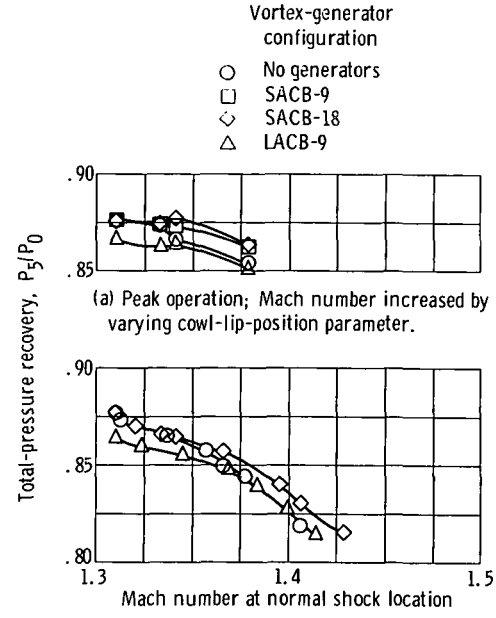

(a) Peak operation; Mach number increased by varying cowl-lip-position parameter.

(b) Design cowl-lip-position parameter; Mach number increased by supercritical operation.

Figure 20. - Effect of aft centerbody vortex-generator configurations on compressor-face total-pressure recovery. Bleed configuration 1.

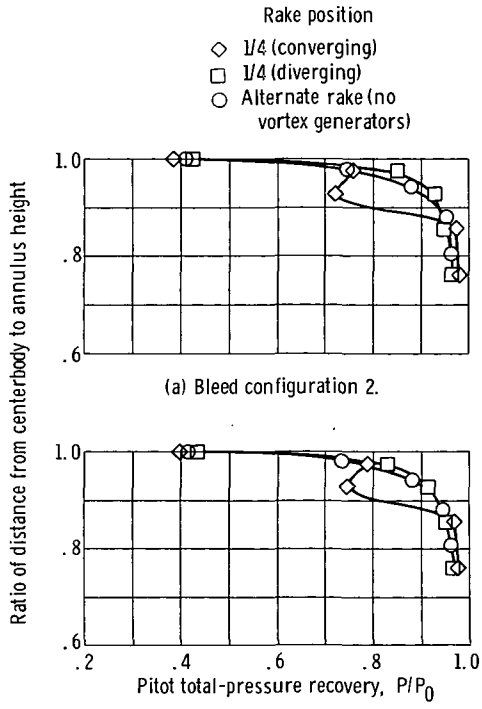

(a) Bleed configuration 2.

(b) Bleed configuration 3.

Figure 21. - Performance of cowl vortex generators C-9 as measured by cowl rakes.

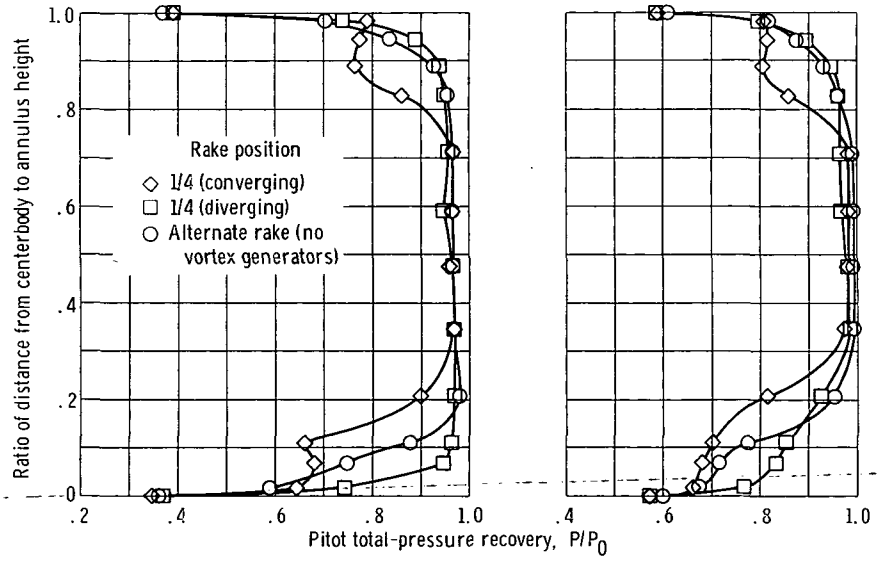

(a) Supercritical inlet operation.

(b) Peak recovery inlet operation.

Figure 22. - Performance of cowl and centerbody vortex-generator configurations C-9 and SACB-9 as measured by throat exit rakes for cowl-lip-position parameter θ_ℓ of 25.26° - bleed configuration 2.

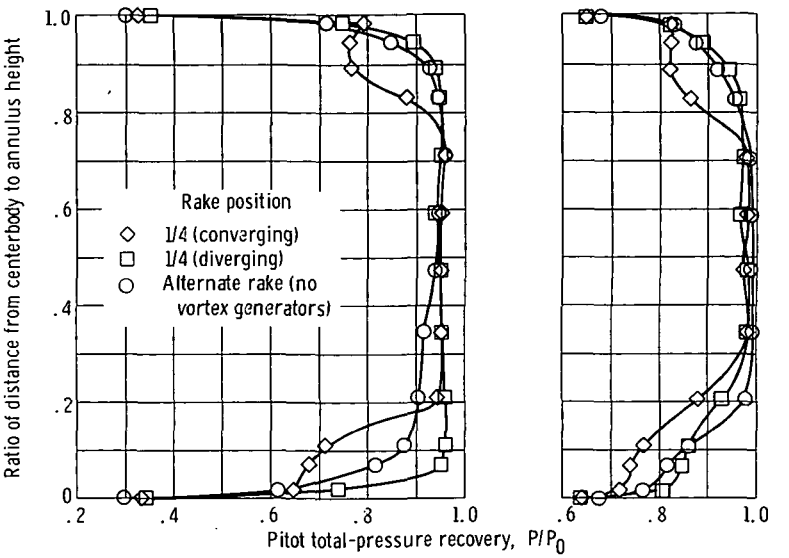

Figure 23. - Performance of cowl and centerbody vortex-generator configurations C-9 and SACB-9 as measured by throat exit rakes for cowl-lip-position parameter θ_l of 25.26° - bleed configuration 3.

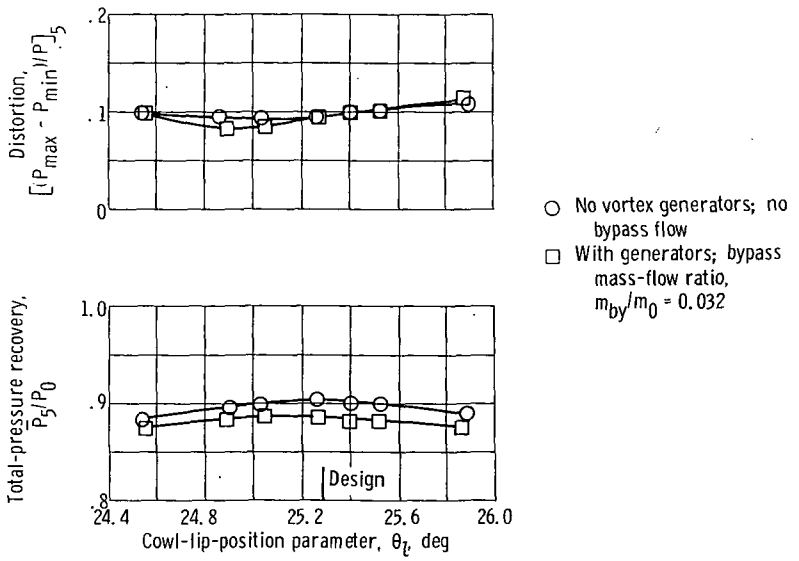

(a) Peak recovery conditions.

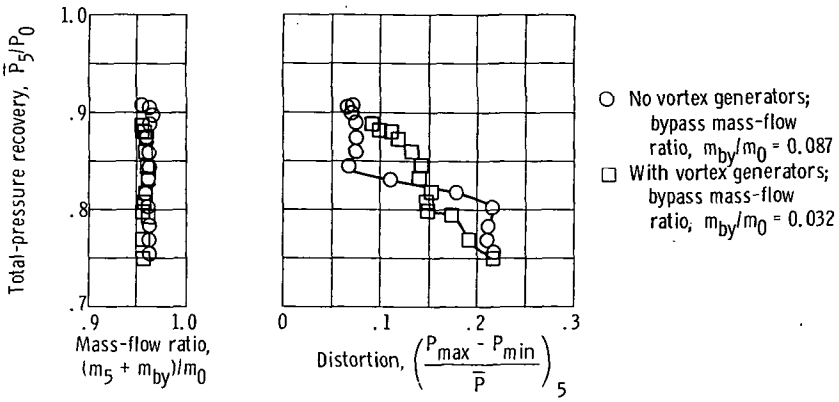

(b) Cowl-lip-position parameter θ_l of 25.26°.

Figure 24. - Effect of cowl and centerbody vortex-generator configurations C-9 and SACB-9 on inlet performance - bleed configuration 2.

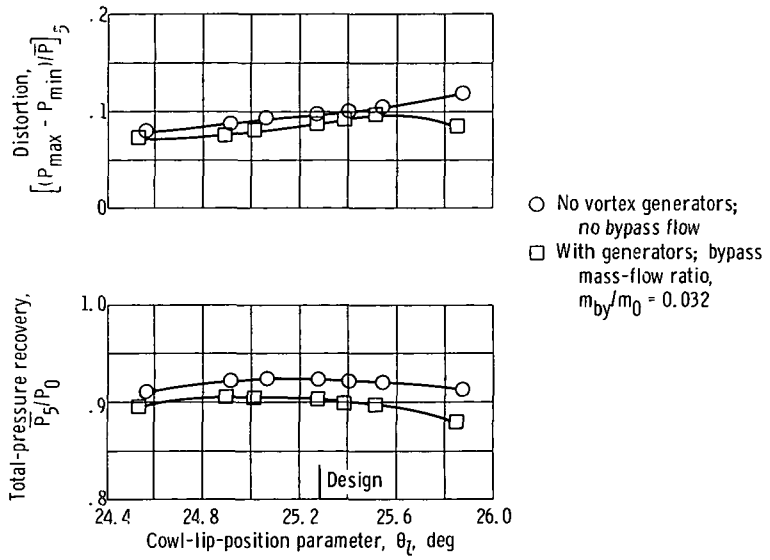

(a) Peak recovery conditions.

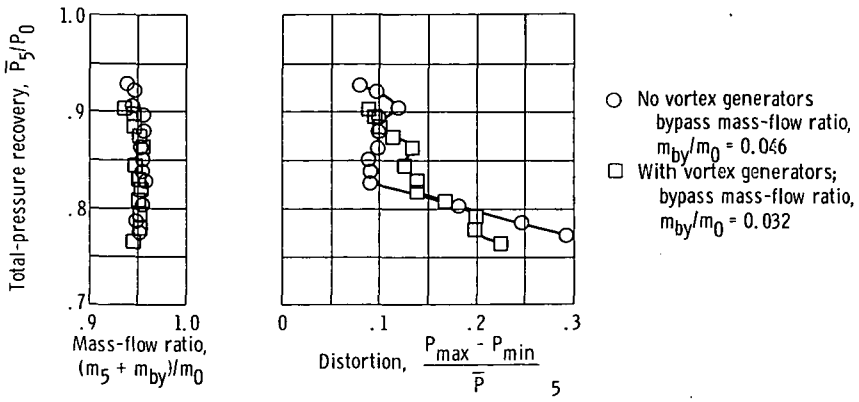

(b) Cowl-lip-position parameter θ_l of 25.26°.

Figure 25. - Effect of cowl and centerbody vortex-generator configurations C-9 and SACB-9 on inlet performance - bleed configuration 3.

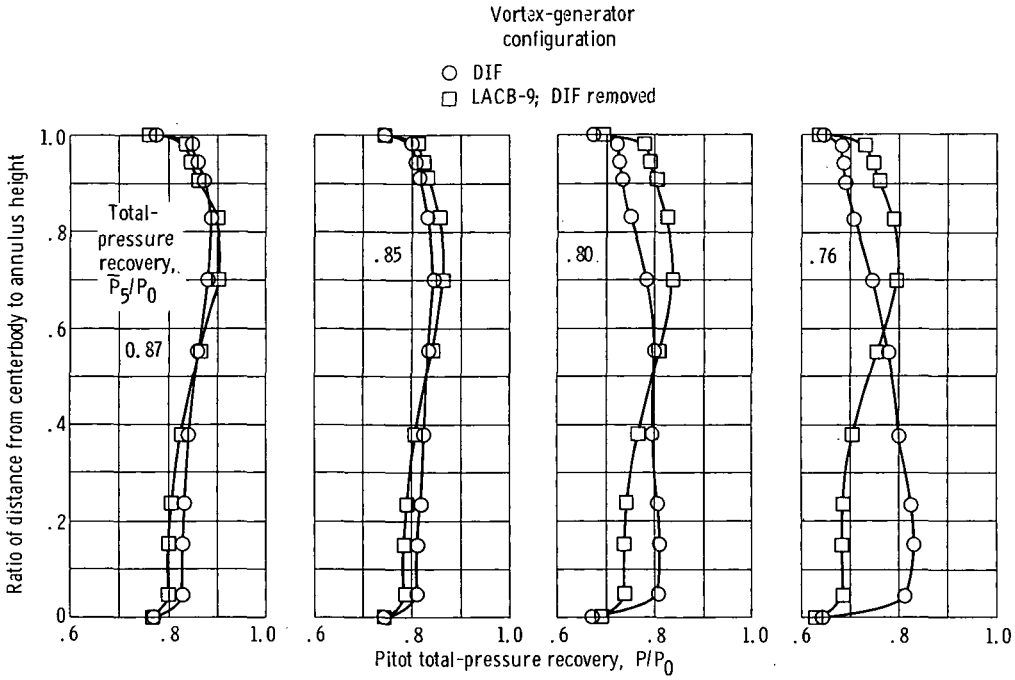

Figure 26. - Performance of centerbody vortex-generator configurations DIF and LACB-9 as measured by compressor-face rakes. Cowl-lip-position parameter θ_l of 25.26°; bleed configuration 1; bleed mass-flow ratio m_{by}/m_0 of 0.032.

NASA-Langley, 1971 —— 1 E-6418

"The aeronautical and space activities of the United States shall be conducted so as to contribute . . . to the expansion of human knowledge of phenomena in the atmosphere and space. The Administration shall provide for the widest practicable and appropriate dissemination of information concerning its activities and the results thereof."

—NATIONAL AERONAUTICS AND SPACE ACT OF 1958

NASA SCIENTIFIC AND TECHNICAL PUBLICATIONS

TECHNICAL REPORTS: Scientific and technical information considered important, complete, and a lasting contribution to existing knowledge.

TECHNICAL NOTES: Information less broad in scope but nevertheless of importance as a contribution to existing knowledge.

TECHNICAL MEMORANDUMS: Information receiving limited distribution because of preliminary data, security classification, or other reasons.

CONTRACTOR REPORTS: Scientific and technical information generated under a NASA contract or grant and considered an important contribution to existing knowledge.

TECHNICAL TRANSLATIONS: Information published in a foreign language considered to merit NASA distribution in English.

SPECIAL PUBLICATIONS: Information derived from or of value to NASA activities. Publications include conference proceedings, monographs, data compilations, handbooks, sourcebooks, and special bibliographies.

TECHNOLOGY UTILIZATION PUBLICATIONS: Information on technology used by NASA that may be of particular interest in commercial and other non-aerospace applications. Publications include Tech Briefs, Technology Utilization Reports and Technology Surveys.

Details on the availability of these publications may be obtained from:

SCIENTIFIC AND TECHNICAL INFORMATION OFFICE

NATIONAL AERONAUTICS AND SPACE ADMINISTRATION

Washington, D.C. 20546